Ferrocenyl Diquat Derivatives: Nonlinear Optical Activity, Multiple Redox States and Unusual Reactivity

Benjamin J. Coe, John Fielden, Simon P. Foxon, Inge Asselberghs, Koen Clays, Stijn Van Cleuvenbergen, and Bruce S. Brunschwig

Supporting Information

1. Additional X-Ray Crystallographic Details

[**3**][PF_6]$_2$•2Me_2CO gave the highest quality structure obtained for a reproducibly prepared material in this study and its geometric parameters (Table S1) are typical of the chromophores described. [**5**][PF_6]$_2$•3MeCN crystallized from acetonitrile (Figure S1). The vinyl C–C distances in this structure, 1.36(1) Å (C11–C12) and 1.34(1) Å (C2–C26), are normal, unlike the unusually short one (1.23(1) Å) in [**5**][PF_6]$_2$•3Me_2CO.

Table S1. Interatomic Distances (Å) and Selected Angles (deg) for the Complex Cation in [3][PF_6]$_2$•2Me_2CO

N1–C8	1.478(4)	C12–C13	1.369(4)	Fe1–C16	2.036(3)
N1–C4	1.366(4)	C14–C15	1.336(4)	Fe1–C17	2.038(3)
N1–C5	1.340(4)	C15–C16	1.452(4)	Fe1–C18	2.040(3)
N2–C7	1.478(4)	C16–C17	1.429(4)	Fe1–C19	2.047(3)
N2–C9	1.353(4)	C16–C20	1.428(4)	Fe1–C20	2.038(3)
N2–C13	1.340(4)	C17–C18	1.410(4)	Fe1–C21	2.043(3)
C1–C2	1.485(5)	C18–C19	1.406(4)	Fe1–C22	2.044(3)
C2–C3	1.390(5)	C19–C20	1.421(4)	Fe1–C23	2.057(3)
C3–C4	1.367(4)	C19–C20	1.414(3)	Fe1–C24	2.037(3)
C5–C6	1.355(5)	C21–C22	1.417(4)	Fe1–C25	2.046(3)
C6–C2	1.400(5)	C21–C25	1.418(5)	C4–C9	1.485(5)
C9–C10	1.371(4)	C22–C23	1.416(4)		
C11–C12	1.399(4)	C23–C24	1.402(4)	C11–C14–C15	127.1(3)
C11–C14	1.441(4)	C24–C25	1.425(4)	C14–C15–C16	124.6(3)

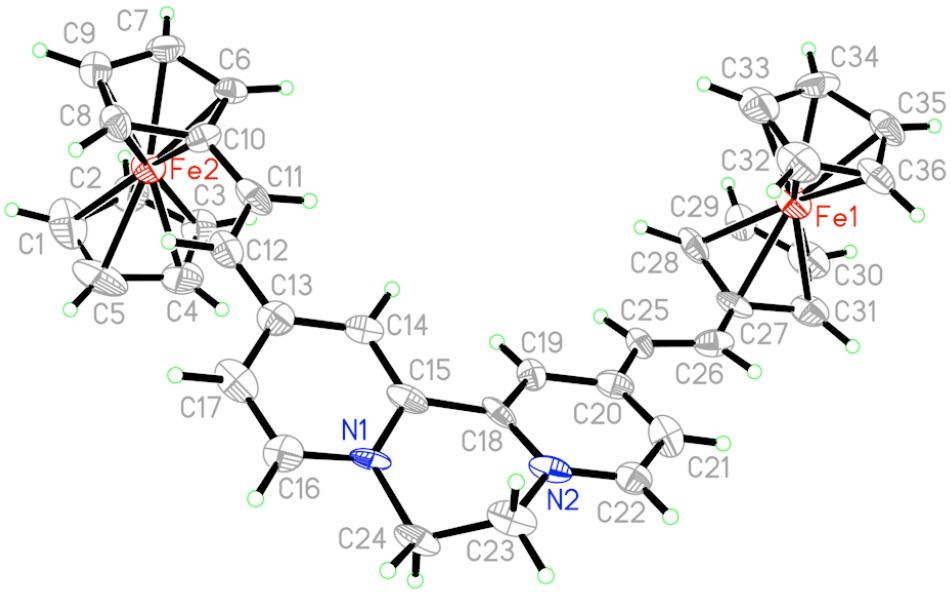

Figure S1. Representation of the molecular structure of the complex cation in [**5**][PF_6]$_2$•3MeCN, with anions and solvent molecules omitted for clarity (50% probability ellipsoids).

Table S2. Crystallographic Data and Refinement Details for [5][PF_6]$_2$•3MeCN and [6][PF_6][OTf]

	[**5**][PF_6]$_2$•3MeCN	[**6**][PF_6][OTf]
formula	$C_{42}H_{41}F_{12}Fe_2N_2P_2$	$C_{38}H_{34}F_9Fe_2N_2O_3PS$
M	1017.44	912.41
cryst syst	triclinic	monoclinic
space group	$P\bar{1}$	$C2/c$
a/Å	10.011(1)	22.257(2)
b/Å	14.438(2)	9.431(1)
c/Å	16.104(2)	18.255(1)
α/deg	73.48(1)	90
β/deg	84.16(1)	112.690(2)
γ/deg	70.41(1)	90
V/Å^3	2102.3(4)	3535.3(5)
Z	2	4
T/K	100(2)	100(2)
μ/mm^{-1}	0.859	1.279
cryst size/mm	0.55 × 0.25 × 0.05	0.09 × 0.06 × 0.01
cryst descript	dark green plate	black block
no. of reflns collected	10826	18726
no. of indep. reflns (R_{int})	7893 (0.0843)	5312 (0.0365)
θ_{max}/deg (completeness)	25.00 (87.4%)	33.63 (98.1%)
reflections with $I > 2\sigma(I)$	3749	4033
goodness-of-fit on F^2	1.007	1.015
final R_1, wR_2 [$I > 2\sigma(I)$]	0.0969, 0.2305	0.0378, 0.0889
(all data)	0.1895, 0.2860	0.0593, 0.0980
peak and hole/eÅ^{-3}	0.964, –0.880	0.557, –0.698

A structure of the mixed salt [**6**][PF_6][OTf] was obtained serendipitously from a crystallization of [**6**][PF_6]$_2$ (diethyl ether vapor diffusion into an acetone solution at room temperature), which clearly still contained traces of triflate anions due to incomplete metathesis. Data were collected by Dr Simon Teat on station 11.3.1 of the Advanced Light Source at Berkeley (synchrotron, λ = 0.77490 Å, Si monochromator). A representation of the molecular structure of the complex cation is shown in Figure S2. This structure has R values lower than for any of the others reported in this work and is of very high resolution. There is a site occupancy disorder between the PF_6^- and OTf^- anions, with both occupying essentially the same position at 50% occupancy. In contrast with [**6**][PF_6]$_2$, [**6**][PF_6][OTf] adopts the centrosymmetric space group $C2/c$ (as for [**5**][PF_6]$_2$•3Me_2CO), so is not expected to show significant bulk NLO effects. Crystallographic data and refinement details for [**5**][PF_6]$_2$•3MeCN and [**6**][PF_6][OTf] are presented in Table S2.

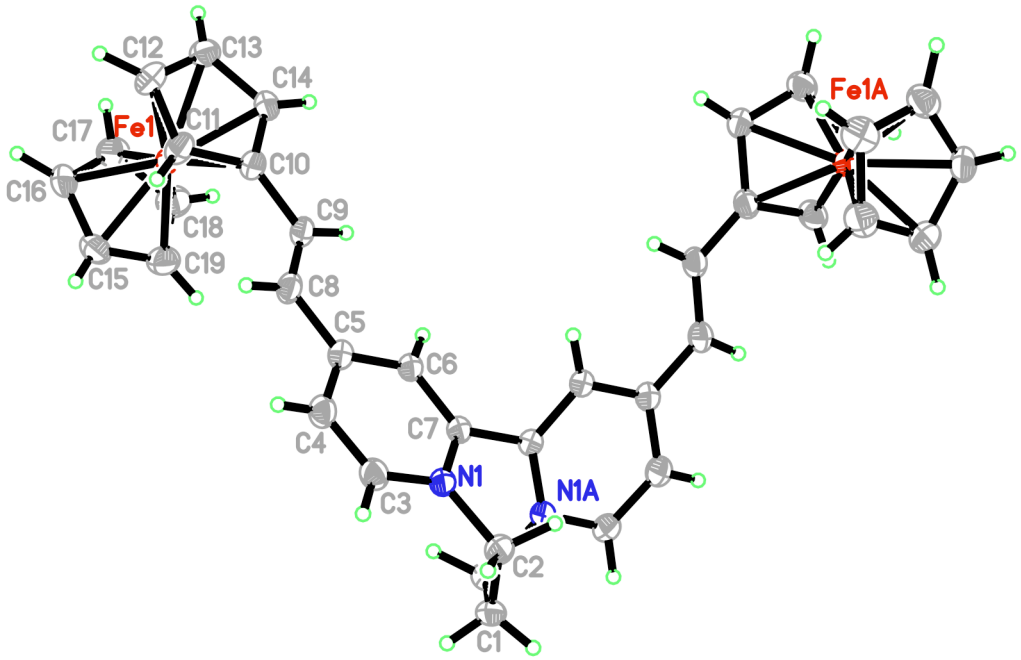

Figure S2. Representation of the molecular structure of the complex cation in [**6**][PF_6][OTf], with anions omitted for clarity (50% probability ellipsoids). Symmetry equivalent carbon atoms are unlabelled.

2. Additional Information Concerning Salt [4b][PF_6]$_4$

Crystals of [**4b**][PF_6]$_4$•4Me_2CO suitable for X-ray diffraction analysis were produced as a trace by-product from an attempted crystallization of [**4**][PF_6]$_2$ from acetone/diethyl ether. Most of the material produced from this crystallization was amorphous [**4**][PF_6]$_2$. While we have been able to reproduce [**4b**][PF_6]$_4$, only very small quantities have as yet been obtained and these are not of analytical purity. The following method was used to afford a sample suitable for ^{1}H NMR and mass spectrometric analysis: [**4**][PF_6]$_2$•0.5Me_2CO (5 mg, 6.74 μmol) was dissolved in acetone (10 mL) and two drops of a dilute HPF_6 solution (0.036% w/v in acetone) were added. Diethyl ether vapor was allowed to diffuse slowly into this solution, producing small quantities of an amorphous green precipitate after 14 d. The mother liquor was separated from the precipitate and more diethyl ether (ca. 10 mL) was added. After another 14 d, a khaki-colored, microcrystalline precipitate was obtained: 2 mg; δ_H (400 MHz, $(CD_3)_2CO$) 9.40 (4 H, d, J = 6.1 Hz, 2C_5H_3N), 8.58 (4 H, s, 2C_5H_3N), 8.23 (4 H, d, J = 6.1 Hz, 2C_5H_3N), 5.42–5.33 (4 H, m, 2NCH_2^{eq}), 4.90–4.78 (4 H, m, 2NCH_2^{ax}), 4.14 (10 H, s, 2C_5H_5), 4.09 (4 H, t, J = 1.9 Hz, 2C_5H_4), 3.95 (4 H, t, J = 1.9 Hz, 2C_5H_4), 3.73 (2 H, q, J = 7.1 Hz, 2CH), 3.62–3.54 (4 H, m, 2CH_2 diastereotopic), 3.52–3.42 (4 H, m, 2CH_2 diastereotopic), 3.28–3.19 (4 H, m, 2CH_2). *m/z* = 1279.6 ([M – PF_6]$^+$), 567.2 ([M – 2PF_6]$^{2+}$), 330.0 ([M – 3PF_6]$^{3+}$).

Studies of the formation of [**4b**]$^{4+}$ suggest that it is acid catalyzed and concentration dependent. Other attempts to reproduce [**4b**][PF_6]$_4$ included treating [**4**][PF_6]$_2$ with base, refluxing a dilute solution of [**4**][PF_6]$_2$ in acetone, and standing more concentrated solutions at room temperature in acetone or acetonitrile. In cases where any reaction occurred, these involved either destruction of the base-sensitive PDQ^{2+} unit or formation of unidentifiable mixtures of Michael-derived oligomers in acetonitrile. These observations contrast with typical base-catalyzed Michael reactions,[1] suggesting that the rate-determining step is transfer of a proton to the vinyl group rather than attack of the activated methyl group. Such reactivity has not been observed in purely organic diquat dervatives, so it may be a consequence of the strong polarization induced in the vinyl unit by the powerful PDQ^{2+} electron acceptor and immediately adjacent Fc donor. A comparable acid-catalyzed, intramolecular nucleophilic attack (by a ketone on an alkyne) was reported recently in another Fc ED–EA system.[2] In that case, the alkyne bridge was also immediately adjacent to both ED and EA groups.

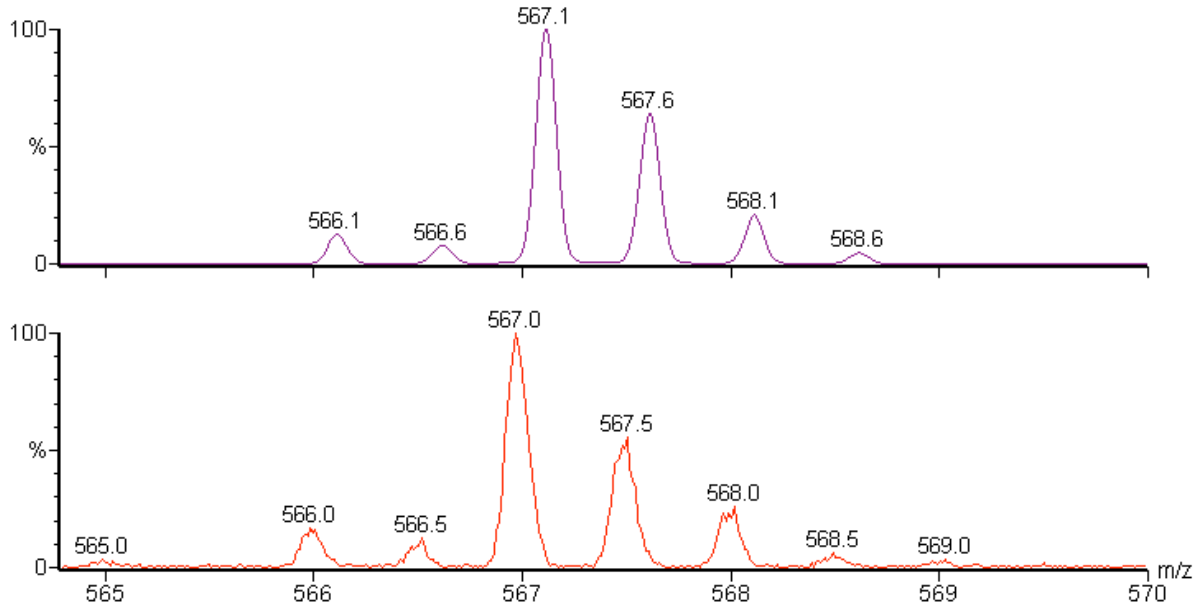

Figure S3. Calculated (top) and experimental (bottom) mass spectra of [**4b**][PF_6]$_4$, showing the peak for ([**4b**][PF_6]$_2$)$^{2+}$ at *m/z* = 567. The *m/z* = 0.5 spacing between the peaks confirms the 2+ charge associated with ([**4b**][PF_6]$_2$)$^{2+}$; by contrast the *m/z* = 567 peak for [**4**][PF_6]$_2$ shows a spacing of *m/z* = 1, corresponding to the singly charged ion pair ([**4**][PF_6])$^{+}$.

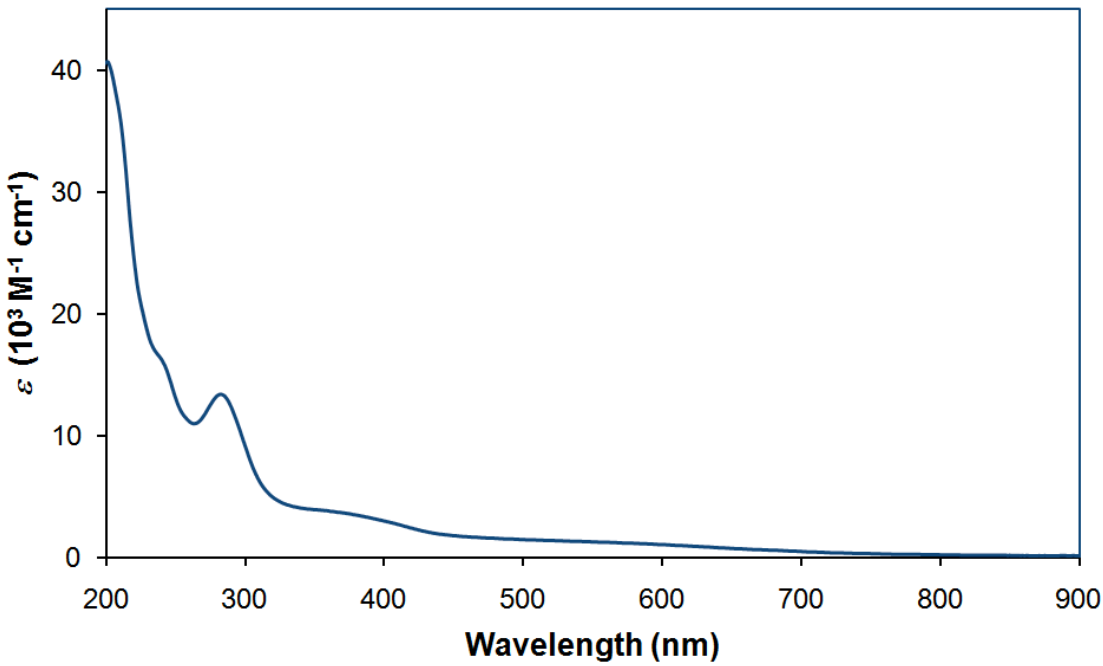

Figure S4. UV–vis absorption spectrum of [**4b**][PF_6]$_4$ at 293 K in acetonitrile (concentration ca. 5×10^{-5} M).

3. UV–Vis Spectroscopy of [3–6][PF_6]$_2$ in Acetone

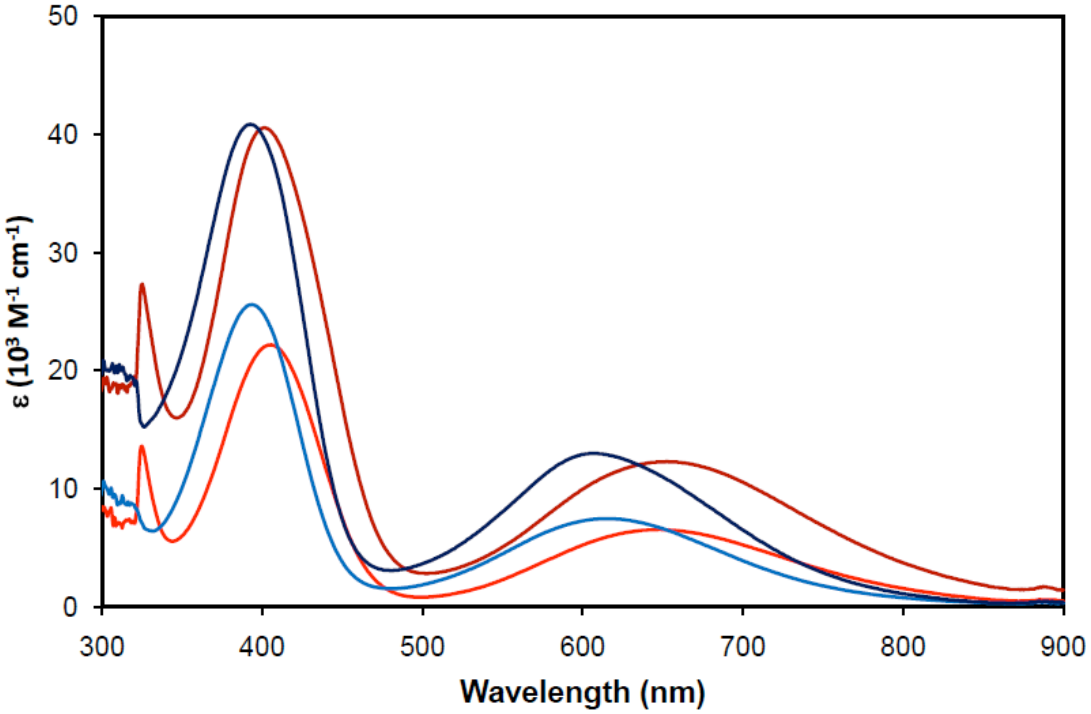

Figure S5. UV–vis absorption spectra of [**3**][PF_6]$_2$ (red), [**4**][PF_6]$_2$ (blue), [**5**][PF_6]$_2$ (dark red) and [**6**][PF_6]$_2$ (dark blue) at 293 K in acetone.

Table S3. UV–Vis Absorption Data for Salts [3–6][PF_6]$_2$ in Acetone[a]

dication	λ_{max}, nm[a] (ε, 10^3 M^{-1} cm^{-1})	E_{max} (eV)	assignment
3	648 (6.5)	1.92	MLCT
	406 (22.0)	3.06	ILCT
4	615 (7.4)	2.02	MLCT
	394 (25.6)	3.15	ILCT
5	657 (12.2)	1.89	MLCT
	401 (40.6)	3.10	ILCT
6	607 (13.0)	2.05	MLCT
	391 (39.5)	3.18	ILCT

[a] Solutions ca. 2–3 × 10^{-5} M.

4. Additional Spectra Measured at 77 K in Butyronitrile

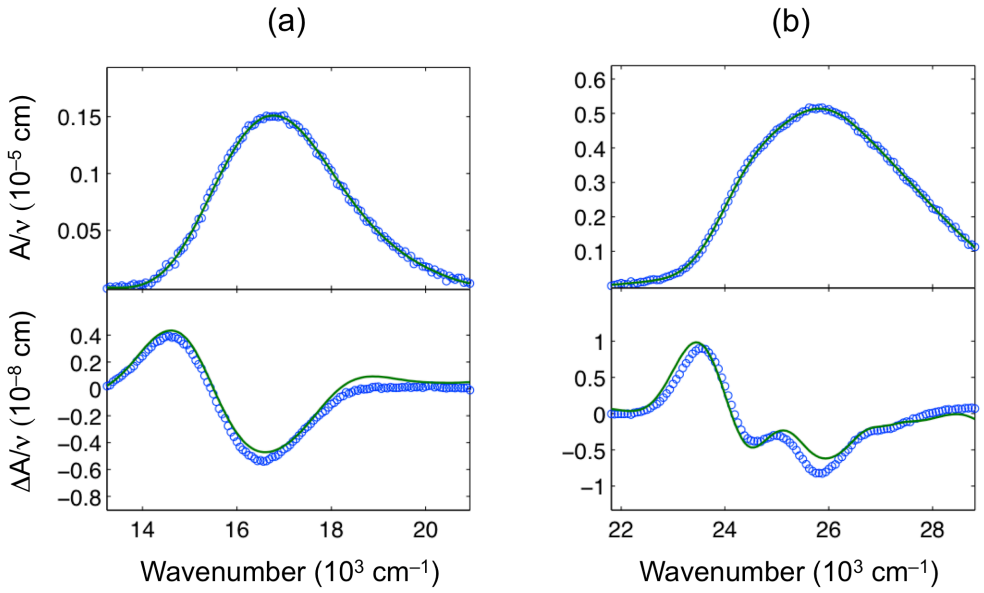

Figure S6. Electronic absorption spectra and calculated fits in the MLCT (a) and ILCT (b) regions for salt [**4**][PF_6]$_2$ in an external electric field of 5.36 × 10^7 V m^{-1}. Top panel: absorption spectrum; bottom panel: electroabsorption spectrum, experimental (blue) and fits (green) according to the Liptay equation.[3]

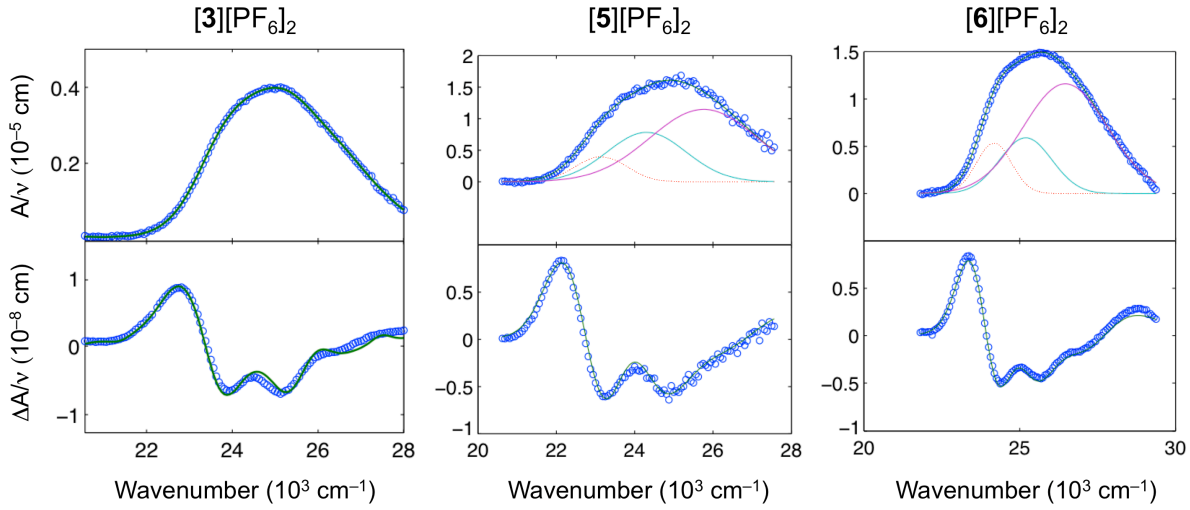

Figure S7. Electronic absorption spectra and calculated fits in the ILCT region for salts [**3**][PF_6]$_2$, [**5**][PF_6]$_2$ and [**6**][PF_6]$_2$ in respective external electric fields of 5.36, 5.26 and 5.36 × 10^7 V m^{-1}. Top panel: absorption spectrum illustrating Gaussian curves used in data fitting for [**5**][PF_6]$_2$ and [**6**][PF_6]$_2$; bottom panel: electroabsorption spectrum, experimental (blue) and fits (green) according to the Liptay equation.[3]

(1) See for example: *March's Advanced Organic Chemistry, 5th Edn*; Smith, M. B.; March, J.; John Wiley & Sons, Inc: New York, 2001.
(2) Kondo, M.; Uchikawa, M.; Kume, S.; Nishihara, H. *Chem. Commun.* **2009**, 1993.
(3) Liptay, W. In *Excited States*, Vol. 1; Lim, E. C., Ed.; Academic Press, New York, 1974, pp. 129–229.